DATA-DRIVEN VIBRATION CONTROL STRATEGY FOR HYPERGRAVITY CENTRIFUGAL SHAKING TABLE

Yang Zhu[1], Xie Haibo[2*]

[1] *State Key Laboratory of Fluid Power and Mechatronic Systems, Zhejiang University, 310058, Hangzhou, Zhejiang, China*
[2] *State Key Laboratory of Fluid Power and Mechatronic Systems, Zhejiang University, 310058, Hangzhou, Zhejiang, China*

* Corresponding author: Tel.: +86 13116788322; E-mail address: hbxie@zju.edu.cn

ABSTRACT

The hypergravity centrifugal shaking table is widely used in the field of civil engineering, which has the scaling effect and is the most effective means of studying the disaster effect of geotechnical earthquake. The compound control of hypergravity centrifugal shaking table is mainly composed of two parts: position servo control and acceleration vibration control. The position servo control is used to ensure that the shaking table works in a safe working area, and the acceleration vibration control is helpful to further improve the seismic wave reproduction ability of the shaking table. Due to the complexity and diversity of the working conditions of the shaking table, it is proved that under the premise of robust position loop control, the vibration control strategy of the acceleration ring of the hypergravity centrifugal shaking table based on the data-driven idea can effectively improve the vibration control accuracy of the hypergravity centrifugal shaking table. At the same time, the vibration control strategy is only based on the current working state of the shaking table. Therefore, It has stronger adaptive control ability.

Keywords: Shaking table, Vibration control, Data-driven, Hypergravity

1. GENERAL INSTRUCTIONS

Earthquake is one of the major natural disasters faced by mankind. It is of great significance to study the earthquake disaster effects such as building damage and sand liquefaction caused by earthquake. Shaking table is a necessary means to study the earthquake disaster effect. The seismic wave generated naturally during the earthquake disaster is a low-frequency elastic wave with a frequency below 10 Hz.

The hypergravity centrifugal shaking table [1, 2] is mainly composed of two parts: a centrifuge that generates an additional heavy force field and an airborne shaking table that is used to reproduce high-frequency seismic waveforms. By using a large centrifuge to attach the heavy force field of the airborne shaking table, the stress equivalence between the scale experiment under hypergravity and the original physical model experiment under normal gravity is realized. Under the action of n g high gravity, the size and vibration duration of the experimental model are reduced by n times, but the vibration frequency and amplitude are also increased by n times.

High-precision seismic signal reproduction is the key technology of airborne shaking table, and it is also the prerequisite for reproducing the real earthquake effect on the corresponding civil structure. The control forms of airborne shaking table are mainly divided into single servo control, vibration control or the combined control strategy of servo control and vibration control. The composite control takes into account the characteristics of good stability of servo control and high precision of vibration

control waveform reproduction, and is an effective means to improve the ability of shaking table waveform reproduction. For servo control, the common control strategy is mainly three-state control [3, 4]. Three-state feedback adjusts the zero position of the system, in which displacement feedback ensures the stability of the system, acceleration feedback improves the damping of the system, and velocity feedback improves the bandwidth of the system. Meanwhile, three-state feedforward is used to eliminate the stable zero near the virtual axis of the system and further improve the bandwidth characteristics of the system. However, different from the executive cylinder of the normal gravity shaking table, which has a long shape path and low natural bandwidth characteristics of the system, the executive cylinder of the high gravity airborne shaking table has a short and thick structure, and its natural bandwidth is high, generally up to about 200 Hz. The system bandwidth is mainly limited by the bandwidth characteristics of the system servo valve. Therefore, the three-state control of the hypergravity airborne shaking table has certain limitations. In terms of vibration control, the relevant adaptive control vibration control strategy [5] and iterative control strategy [6] are more actively studied, but their research objects are mainly aimed at the normal gravity shaking table condition, and the vibration control strategy of the airborne shaking table with hypergravity needs to be further studied and verified.

This paper mainly includes the following parts, the second part is the schematic description and the dynamic modeling of airborne shaking table, the servo control and vibration control strategy of the hypergravity airborne shaking table as the third part, the fourth part is the simulation and experimental results, and the fifth part is conclusion.

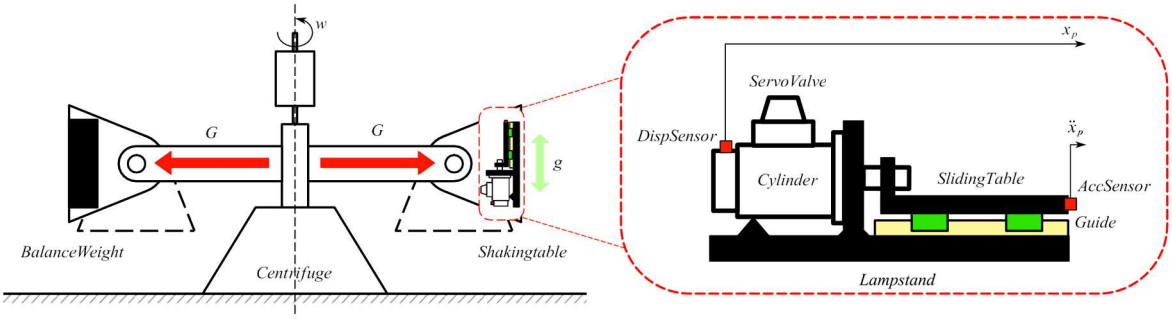

Figure 1: Hypergravity unidirectional centrifugal shaking table structure

2. SYSTEM ANALYSIS

2.1. Physical system

The hypergravity centrifugal shaking table system is shown in Figure 1, which is mainly composed of two parts: centrifuge system and unidirectional airborne shaking table.

Centrifuge rotates at a high speed under the action of the driving motor to generate centrifugal force G with a specific gravity value. The unidirectional airborne shaking table is installed in the basket on one side of the centrifuge, and the basket on the other side is the centrifuge counterweight. The direction of the vibration acceleration g of the unidirectional airborne shaking table is perpendicular to the centrifugal force G and is naturally decoupage. Under this premise, in order to facilitate the study of the hypergravity centrifugal shaking table, the unidirectional shaking table studied here is in the normal gravity environment. The study of the high-frequency vibration characteristics of the airborne shaking table in the normal gravity environment is equivalent to the study of the airborne shaking table in the actual heavy force field.

2.2. System analysis and modelling

The schematic of the airborne shaking table system is shown in Figure 2, which is a typical single-cylinder double-valve system. The purpose of the dual valve parallel [7] is to consider that the main factor affecting the bandwidth of the unidirectional airborne shaking table system is the bandwidth characteristics of the servo valve. The higher bandwidth characteristics of the servo valve often correspond to the working condition of the servo valve small opening, that is, the working condition of the servo valve small flow rate. When the double valves are in parallel, the demand flow rate of the single valve is reduced by half theoretically, so the double valves in parallel can greatly improve the bandwidth characteristics of the system.

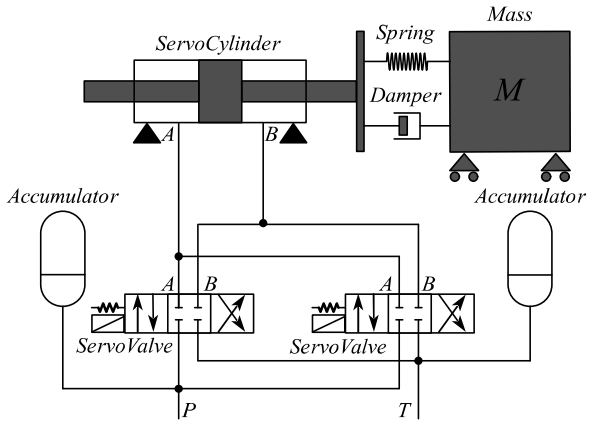

Figure 2: Schematic of unidirectional airborne shaking table

The load force balance equation for the single-cylinder double-valve system is established as shown in equation (1):

$$A_p P_L = m\frac{d^2x_p}{dt^2} + B_p\frac{dx_p}{dt} + F_L \tag{1}$$

where, A_p is the actuating area of the cylinder, m is the mass of the piston and load converted to the load rod, x_p is displacement, B_p represents the viscous damping coefficient, F_L is the accidental load force, P_L is the load pressure. The continuity equation of the flow is established as follows (2):

$$Q_L = A_p\frac{dx_p}{dt} + \frac{V_t}{4\beta_e}\frac{dP_L}{dt} + C_{tp}P_L \tag{2}$$

where, Q_L represents the system load flow rate, V_t represents the total volume of the cylinder and the pipeline between the cylinder and the servo valve, β_e represents the effective bulk elastic modulus, the linear equation of the servo valve flow rate is shown in equation (3):

$$Q_L = K_q x_v + K_c P_L \tag{3}$$

K_q is the flow coefficient, K_c is the flow pressure coefficient of the servo valve, and x_v is the spool displacement of the servo valve. Let $K_{cy} = \frac{K_q}{A_p}$ indicate the system open-loop gain, $K_{ce} = K_c + C_{tp}$ indicate the total flow pressure coefficient, and $C_{tp} = C_{ip} + \frac{C_{ep}}{2}$ indicate the total leakage coefficient, $w_h = \sqrt{\frac{4\beta_e A_p^2}{V_t m}}$ and $\xi_h = \frac{K_{ce}}{A_p}\sqrt{\frac{\beta_e m}{V_t}}$ respectively represent system natural frequency and the hydraulic

damping ratio. Considering that the load viscous damping coefficient B_p is small, meet $\frac{K_{ce}B_p}{A_p^2} \ll 1$. Connected equations (1-3), the transfer function of single cylinder double valve can be obtained as follows (4):

$$X_p = \frac{K_{cy}}{s(\frac{s^2}{w_h^2} + \frac{2\xi_h}{w_h}s + 1)} X_v \tag{4}$$

The two-valve parallel dynamic model can be approximately simplified into a second-order oscillation system as shown in equation (5):

$$X_v = \frac{K_{sv}}{\frac{s^2}{w_{sv}^2} + \frac{2\xi_{sv}}{w_{sv}}s + 1} U \tag{5}$$

where, K_{sv} is the gain coefficient of dual valves in parallel, w_{sv} is the servo bandwidth and ξ_{sv} is the damping coefficient. The dynamic model of shaking table can be obtained by connecting equations (4-5), as shown in equation (6):

$$X_p = \frac{K_s U}{s\left(\frac{s^2}{w_h^2} + \frac{2\xi_h}{w_h}s + 1\right)(\frac{s^2}{w_{sv}^2} + \frac{2\xi_{sv}}{w_{sv}}s + 1)} \tag{6}$$

where, $K_s = K_{cy}K_{sv}$ represents the total open-loop gain of the system.

3. ALGORITHM DESIGN

3.1. Servo control strategy

Due to its inherent limitations, the single degree of freedom controller cannot meet the control requirements of tracking and disturbance rejection at the same time, and the single degree of freedom controller must make a compromise between these two performance objectives, while the two degrees of freedom controller fundamentally overcomes the inherent defects of the single degree of freedom controller, and has two degrees of freedom to handle disturbance rejection and tracking tasks separately 0. Based on the displacement feedback signal, a controller with two degrees of freedom is established as the servo controller of the airborne shaking table. While ensuring the sufficient robustness of the shaking table displacement ring, the displacement control accuracy of the shaking table is improved as much as possible, thus laying the foundation for the high-precision control of the acceleration of the shaking table. The servo control frame of the airborne shaking table is shown in Figure 3:

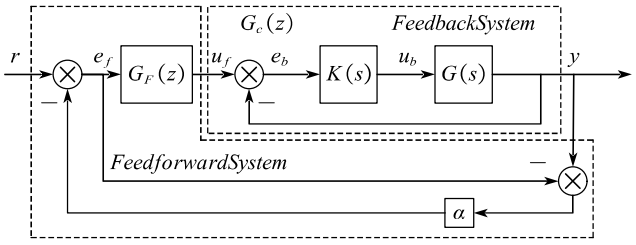

Figure 3: Servo control frame of unidirectional airborne shaking table

where, the system transfer function model G(s) and the feedback controller K(s) designed based on H_∞ method 0 constitute airborne shaking table displacement closed loop. Further, the nominal model $G_c(z^{-1})$ of the system position closed loop is determined through identification experiments. The feedforward controller $G_F(z) = G_c^{-1}(z)F(z)$ in the system is constructed by using the improved internal model control strategy 0, where $G_c^{-1}(z)$ and F(z) represent the nominal inverse model of the system 0 and the low-pass filter to prevent the system's high-frequency gain from being too large, respectively. $0 < \alpha < 1$ is the gain factor in the improved internal model controller.

3.2. Vibration control strategy

Under a single servo control link, the accuracy of acceleration seismic reproduction is often difficult to meet the application requirements. The main reasons are that firstly, the actual acceleration signal is deviated from the theoretical displacement corresponding to the corresponding acceleration, which is obtained by integrating the input servo link twice. Secondly, the vibration components of the shaking table are not completely rigid. Elastic deformation will occur and the installation and connection of each component will inevitably leave a gap. The existence of the above factors makes the acceleration signal in the high-frequency vibration of the shaking table subject to obvious harmonic interference. Therefore, only a single servo control strategy can not meet the high-precision reproduction of the acceleration waveform of the shaking table. The data-driven vibration control frame of the airborne shaking table is shown in Figure 4:

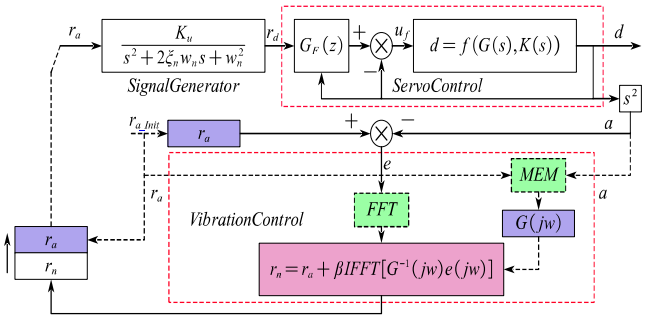

Figure 4: Vibration control frame of unidirectional airborne shaking table

where, the acceleration reference signal r_a generates the corresponding displacement signal r_d after passing through the second-order signal generator. Under the action of the servo control link, the shaking table completes the excitation experiment and collects the acceleration signal generated by the current excitation experiment at the same time. The vibration controller uses the corresponding input and output signals and uses the maximum entropy method 0, to obtain and save the frequency response of the system acceleration ring, and updates the new control input signals according to equation (7, 8):

$$r_n = r_a + \beta IFFT[G^{-1}(jw)\mathrm{e(jw)}] \tag{7}$$

$$\mathrm{e(jw)} = \mathrm{FFT}(r_a - a) \tag{8}$$

where $0 < \beta < 1$. The acceleration signal of the control input is iteratively optimized by data-driven method, and then the accuracy of the random acceleration signal of the shaking table is improved. For the airborne shaking table system, set the frequency response as G, random process input as x(n), output as y(n), and sequence length as N, then $\mathrm{G}(f) = \sqrt{\frac{P_{yy}(f)}{P_{xx}(f)}}$ in the frequency domain. $P_{yy}(f)$ and $P_{xx}(f)$ represent the self-power spectrum of the output signal and the input signal respectively. In the traditional spectral estimation method, it is assumed that when $n \geq N$, the autocorrelation of the signal is zero. In many cases, the above assumption is not true, so the resolution and accuracy of the

estimated spectrum will be significantly reduced by this window method. The maximum entropy method is a nonlinear spectral estimation method which can obtain high resolution by extrapolating the autocorrelation function at the known finite delay point according to the maximum entropy criterion.

It is especially suitable for spectral estimation of short data series. Based on this, the maximum entropy method is used to estimate the frequency response of the airborne shaking table acceleration ring during the implementation of vibration control strategy.

4. SIMULATION AND EXPERIMENT

4.1. System identification and simulation

The structure of the unidirectional airborne shaking table is shown in Figure 5. Under the joint action of the relief valve and the accumulator, the system works in a stable pressure environment as far as possible. The double valve parallel system can ensure that the flow supply of single valve is reduced under the same flow demand of the system, and then effectively improve the bandwidth characteristics of the airborne shaking table system. At the same time, the inertial load with a mass of 82 kg is installed on the surface of the airborne shaking table.

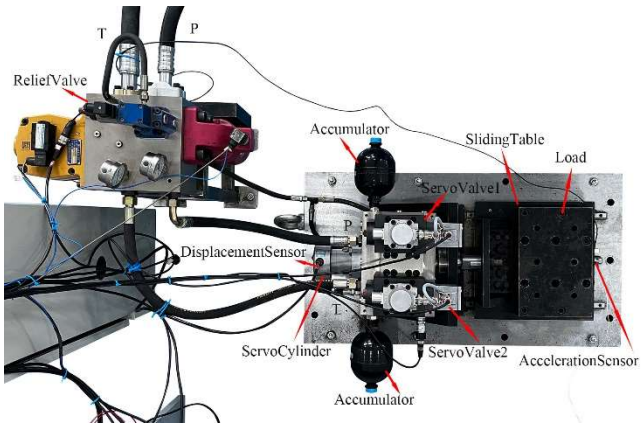

Figure 5: Mechanical structure of unidirectional airborne shaking table

Specific identification experiments are carried out on unidirectional airborne shaking table, and the transfer model of unidirectional airborne shaking table can be obtained as follows (9):

$$\hat{G}(s) = \frac{2.002e13}{s^5 + 1188s^4 + 513400s^3 + 2.362e08s^2 + 3.084e10s} \tag{9}$$

Analyze and compare the step response of the system model and the actual step response of the system, and then verify the effectiveness of the identification model. The specific comparison results are shown in Figure 6.

As can be seen from Figure 6, the 5th-order transfer function model of the system obtained by the identification experiment can better fit the step response of the actual system, and has sufficient system identification accuracy.

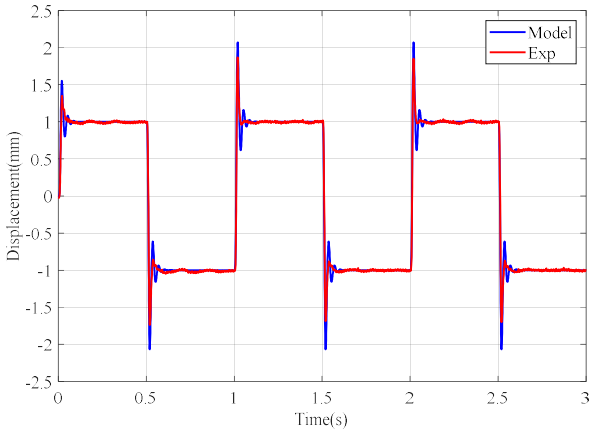

Figure 6: The open loop identification result of displacement of airborne shaking table

4.2. Experimental results

According to the displacement open-loop model, the servo controller of the airborne shaking table is designed. The displacement reference signal is obtained by integrating the corresponding random seismic acceleration signal twice. The specific expressions of the servo controller are shown in equations (10-12):

$$K(s) = \frac{\begin{array}{c}806.1s^4 + 4.403\text{e}05s^3 + \\ 2.451\text{e}08s^2 + 6.718\text{e}10s \\ +6.323e9\end{array}}{\begin{array}{c}s^5 + 1265s^4 + 1.18\text{e}06s^3 + \\ 3.952\text{e}8s^2 + 2.12\text{e}11s \\ +1.8e11\end{array}} \tag{10}$$

$$G_c^{-1}(z) = \frac{\begin{array}{c}(z-0.9776)(z-0.7507) \\ (z^2-1.585z+0.7567) \\ (z^2+1.126z+0.751) \\ (z^2-0.5812z+0.7312) \\ (z^2+0.2856z+0.7664)\end{array}}{\begin{array}{c}0.011534z(z-0.9807) \\ (1.494z^2+2.339z+1) \\ (1.122z^2-1.159z+1) \\ (1.299z^2+1.362z+1) \\ (1.122z^2-0.2889z+1)\end{array}} \tag{11}$$

$$F(z) = \frac{0.5887z + 0.2574}{z^2 - 0.2924z + 0.1085} \tag{12}$$

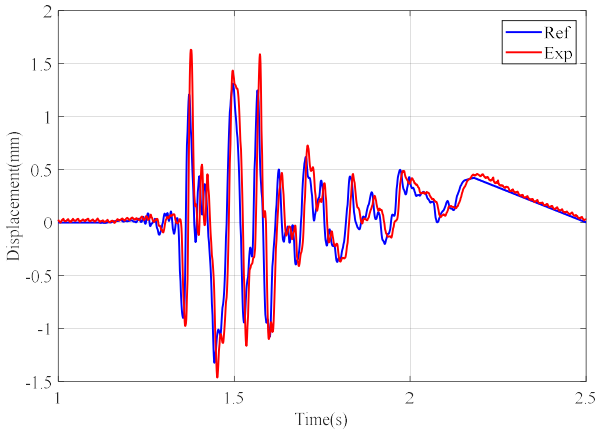

Figure 7: Input and output waveform of random seismic displacement signal on unidirectional airborne shaking table

Figure 7 shows that under the action of the servo controller, where $\alpha = 0.2$. the displacement ring of the shaking table can have a high displacement reproduction accuracy while ensuring the stability of the system. Under the premise of closed-loop displacement of the system, the input and output signals of random acceleration signal are collected, and the maximum entropy method (MEM) is used to identify the system in the frequency domain, and the corresponding system frequency response is obtained as shown in Figure 8.

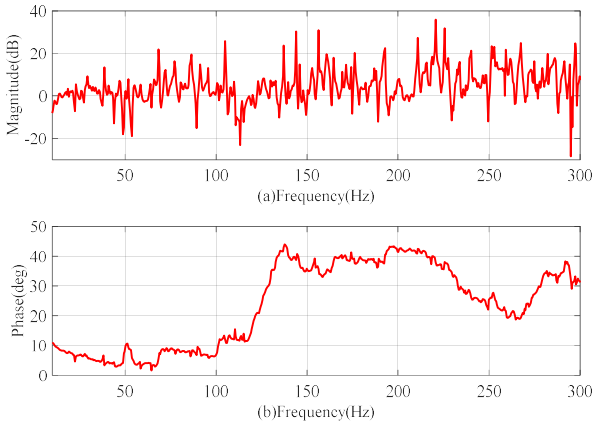

Figure 8: Frequency response of unidirectional airborne shaking table acceleration ring

In order to verify the effectiveness of the vibration strategy proposed here, the same random seismic signal is used for experiments under the two conditions of only servo control and the combination of servo and vibration control. The experimental results are shown in Figure 9.

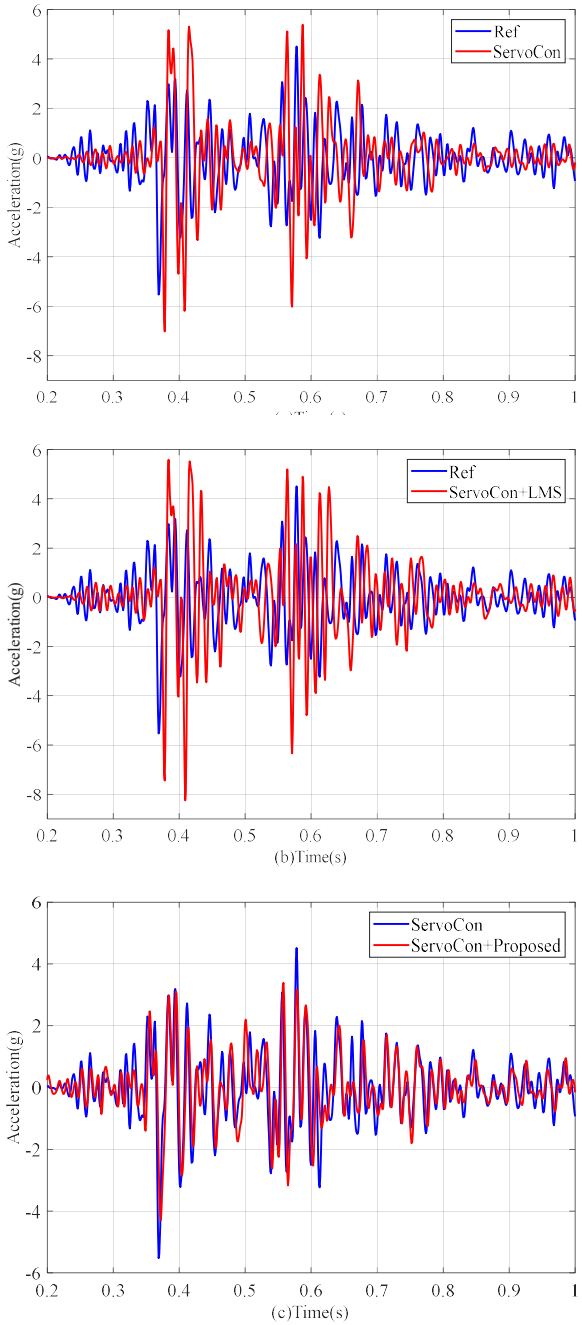

Figure 9: Input and output waveform of random seismic signal airborne shaking table

Figure 9 respectively shows the comparison between the output acceleration waveform and the reference acceleration waveform of the airborne shaking table under the same acceleration input in three cases. Figure (a): Only two degrees of freedom servo control strategy is used; Figure (b): On the basis of the servo control strategy, a vibration control strategy based on LMS 0 is further introduced, where $\mu = 0.001$; Figure (c): A data-driven vibration control strategy is introduced based on servo control measurements, where $\beta = 0.5$. Compared with the above three figures, it is found that the vibration control strategy based on data drive can obviously improve the reproduction accuracy of the acceleration waveform of the airborne shaking table under the same servo control.

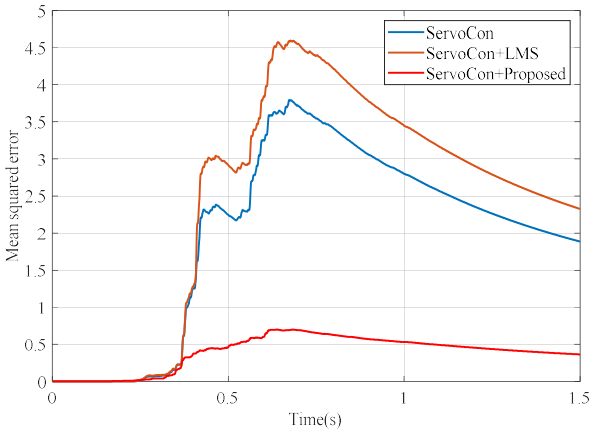

Figure 10: MSE comparison of input and output waveforms of random seismic signal airborne shaking table

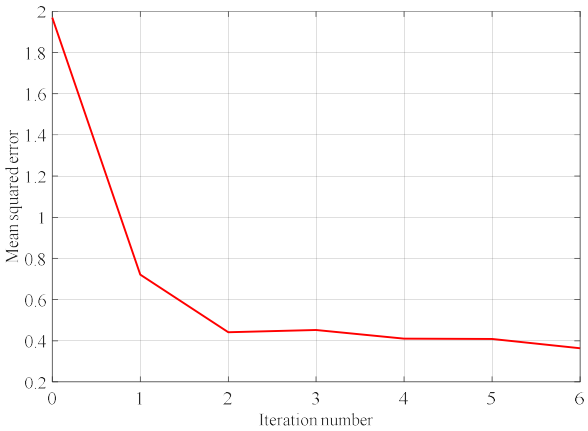

Figure 11: Global MSE iteration trend chart

The following conclusions can be drawn from the analysis of Figure 10 and Figure 11:(1) Compared with a single servo control strategy, only the combination of appropriate vibration control strategy and servo control strategy can further improve the accuracy of acceleration waveform reproduction of the shaking table; (2) Under the same servo control link, the proposed shaking table vibration control strategy, after a certain number of iterative optimization, can effectively improve the acceleration waveform reproduction accuracy of the shaking table, and it is iteratively converging.

5. CONCLUSION

In this paper, taking the hypergravity centrifugal shaking table as the research object, the problem of the poor reproduction accuracy of the acceleration waveform of the airborne shaking table under the action of a single servo controller is studied. When an airborne shaking table operates under a single servo controller, the reproduction accuracy of the shaking table acceleration waveform is often poor due to the deviation of the displacement signal obtained by the double integration of theoretical acceleration, the finite stiffness of the shaker table and the existence of installation gap. Based on this, a data-driven vibration control strategy for airborne shaking table is proposed, and the corresponding vibration control strategy is introduced into the airborne shaking table control system on the basis of servo control. The final experimental results show that the proposed vibration control strategy can effectively improve the acceleration waveform reproduction accuracy of airborne shaking table. At the same time, the proposed vibration control strategy is compared with the existing vibration optimization control strategy based on LMS, which further verifies the advanced nature of the proposed vibration control strategy.

REFERENCES

[1] Zhou, Y. G., Meng, D., Ma, Q., Ling, D. S. (2020). Frequency response function and shaking control of the ZJU-400 geotechnical centrifuge shaker. *International Journal of Physical Modelling in Geotechnics*, *20*(2), 97-117.

[2] Hung, W. Y., Liang, Y. C., Huang, J. X., & Pham, T. N. P. Effect of soil particle size on seismic response of gentle slope by centrifuge shaking table test.

[3] Qianli, L., Zhangwei, C., & Jinrong, X. (2014). Three-variable control technique for a seismic analog shaking table. *Journal of Vibration and Shock*, *33*(8), 54-60.

[4] Luan, Q. L., Chen, Z. W., Xu, J. R., & He, H. N. (2014). Three-variable control parameter tuning technology on seismic simulation shaking tables. *Journal of Vibration Engineering*, *27*(03), 416-425.

[5] Shen, G., Li, X., Zhu, Z., Tang, Y., Zhu, W., & Liu, S. (2017). Acceleration tracking control combining adaptive control and off-line compensators for six-degree-of-freedom electro-hydraulic shaking tables. *Isa Transactions*, *70*, 322-337.

[6] Tang, Y., Shen, G., Zhu, Z. C. (2014). Time waveform replication for electro-hydraulic shaking table incorporating off-line iterative learning control and modified internal model control. *Proceedings of the Institution of Mechanical Engineers, Part I: Journal of Systems and Control Engineering*, *228*(9), 722-733.

[7] Bai, Y., & Quan, L. (2016). Improving electro-hydraulic system performance by double-valve actuation. *Transactions of the Canadian Society for Mechanical Engineering*, *40*(3), 289-301.

[8] Pal, M., Sarkar, G., Barai, R. K. (2019). Two-Degree-of-Freedom Control of Non-minimum Phase Mechanical System. In *Modelling and Simulation in Science, Technology and Engineering Mathematics: Proceedings of the International Conference on Modelling and Simulation (MS-17)* (pp. 365-378). Springer International Publishing.

[9] Shiralkar, A., Kurode, S., Gore, R., & Tamhane, B. (2019). Robust output feedback control of electro-hydraulic system. *International Journal of Dynamics and Control*, *7*, 295-307.

[10] Huang, L., Pei, H., & Cheng, Z. (2023). System identification and improved internal model control for yaw of unmanned helicopter. *Asian Journal of Control*, *25*(2), 1619-1638.

[11] Rigney, B. P., Pao, L. Y., & Lawrence, D. A. (2009). Nonminimum phase dynamic inversion for settle time applications. IEEE Transactions on Control Systems Technology, 17(5), 989-1005.

[12] Tanc, A. K. (2010). Iterative maximum entropy power spectrum estimation for multirate systems. *AEU-International Journal of Electronics and Communications*, *64*(2), 93-98.

[13] Ferrante, A., Pavon, M., & Zorzi, M. (2011). A maximum entropy enhancement for a family of high-resolution spectral estimators. *IEEE Transactions on Automatic Control*, *57*(2), 318-329.